

THEMAL FLUID FINITE ELEMENT CALCULATIONS FOR THE EUROPEAN PPCS DIVERTOR CONCEPTS

Panos J Karditsas and Neill P Taylor
EURATOM/UKAEA Fusion Association, Culham Science Centre, Abingdon, Oxfordshire, OX14 3DB, UK.

ABSTRACT

As part of the European Power Plant Conceptual Study, two different divertor designs were proposed, based on previous work on HETS (High Efficiency Thermal Shield) performed at FZK and ENEA. The coolant is helium gas at pressures in the range 10-14 MPa and the inlet temperatures are in the range of 500-800°C. The geometrical complexity of the designs made prediction of heat transfer coefficients, needed for conducting thermal and structural analysis, difficult, and the calculated values from empirical correlations uncertain. This paper presents and summarises results of thermal-fluid calculations performed on both divertor concepts and gives estimates of effective values of heat transfer coefficients based on the local flow conditions and temperature distributions. The agreement of calculations with experimental values for similar conditions, inspires confidence in results from such calculations, and demonstrates that computational fluid dynamic finite element codes can accurately predict behaviour, and can be used to optimise the designs.

I. INTRODUCTION

Divertor design concepts were studied as part of the European Power Plant Conceptual Study, which started in 2000. Primary requirements were operation with helium, so that high temperatures can be realised for better power plant thermodynamic efficiency, and the ability to withstand 10 MW/m² of incident flux.

Two designs based on previous work on HETS, the High Performance Thermal Shield, performed at FZK and ENEA were proposed and studied. Details of the designs can be found in previous reports^{1,2}. Schematic cut-away sections of these designs, used in this study for the finite element calculations are shown in Figs. 1-2. The basic feature of both designs is flow of coolant at high speed through a narrow channel of width in the range 0.9-2mm, and the use of tungsten as the pressure retaining and armour material.

Finite element calculations were performed on sections of the proposed divertor designs, using the commercially available fluid dynamics code FlowPlus, the fluid module of the COSMOS/M(2.6)⁷ family of solvers.

II. GENERAL DESIGN FEATURES

The divertor plate and armour should be capable of withstanding a flux of 10MW/m² and the structure made of tungsten must operate well below its melting point of 3660K. The properties of tungsten and helium used for calculations are from reference 3.

Design 1, shown in Fig. (1), is symmetric around the vertical y-direction. Flow goes through a narrow gap, impinges on the heated part of the structure, side (AB)=12mm, and then is diverted sideways through a narrow channel of 1mm height, lined with 1mm diameter pins, depicted by the shaded area between locations P2 and P4 in Fig. (1). The length of the narrow channel lined with the pins is 5mm. The pin material is tungsten.

The design originally assumed a helium inlet temperature of 700°C, did not include lining with pins, the channel height was 0.1mm, and the requirement was for flow velocities of ~200m/s, to achieve heat transfer coefficient values of 30,000W/m²-K. This was necessary for adequate heat removal to keep the structural temperature at acceptable levels. Thermal-fluid dynamic analysis confirmed that the values of heat transfer assumed in the thermal studies were in good agreement with calculations, and the experimental and calculated structure temperatures were within 50K.

The objective of the revised design was to achieve the highest possible heat transfer by increasing the contact between the top heated region of the structure and the lower cooler regions, and simultaneously obtain high heat removal rates by the helium coolant by increasing the fluid-solid contact surface area. This led to lining the channel with pins as previously described: heat is

transferred away from the hot plate (top) by conduction to the cooler parts of the structure, and by convection from the pin and plate surface to the coolant. The inlet temperature is 500°C, pressure 10MPa, and velocity 2.1m/s, resulting in a mass flow rate of 0.09kg/s.

The region lined with pins, in FlowPlus is dealt with by the method of distributed resistances⁴. For geometries with numerous flow obstacles, as in this case the equivalent of tube banks, the obstacles are modelled on the larger scale and are represented by a sink term in the momentum equations. There are several options available in the solver, but the form chosen for calculations is the friction factor method, where the excess pressure gradient is written as:

$$\frac{\partial p_i}{\partial x_i} = \frac{f}{D_H} \left(\frac{\rho V_i^2}{2} \right) \quad (1)$$

The friction factor equation for flow in tube banks⁵ is used, and after adjusting the expression to account for the Reynolds number based on the maximum velocity achieved in the passages between pins, the resulting expression to be used in equation (1), for the 60° staggered pin array, is:

$$f = \frac{D_H}{L} (4Nf') = 39.2 Re_d^{-0.16} \quad (2)$$

with f' the friction factor for staggered tube banks⁵, D_H the pin hydraulic diameter, N the number of pin rows, d the pin diameter and L the length of the region lined with pins. The velocity of helium in the passages between pins is assumed here to be no more than ~72m/s.

Design 2, shown in Fig. 2, is axisymmetric around the vertical y-direction. The design was originally developed for low temperature operation with pressurised water as the coolant, and tests were carried out⁶ that demonstrated capability to withstand ~40MW/m² of incident flux. Experimental results were also corroborated by thermal-fluid finite element calculations, with excellent agreement of structural temperature and flow velocity values.

In the experiments, pressurised water at 1 MPa, 50 C, flows inside a nozzle at 10 m/s, impinges on a hemispherical dome and then is diverted away through a narrow passage. Calculations, using the steam tables for pressurised water properties and quality, showed the flow speeding to ~20 m/s in the narrow passage, and being almost stagnant at the dome top. The experiments demonstrated the divertor could operate stably (without burnout) at a maximum heat flux of ~40 MW/m², resulting in maximum temperatures of ~425°C. Computational fluid dynamic finite element calculations predicted maximum

temperatures of 450°C, and a maximum value for steam/water quality of ~40%. The flow velocity magnitude in the narrow passage was calculated to be 20.2m/s, again in excellent agreement with experimental values.

The design dimensions of this concept were revised to allow for helium cooling. Two cases were investigated, with helium inlet temperatures 800°C (case 2a) and 600°C (case 2b), velocity 200m/s, and pressure 14MPa, with a resulting mass flow of 0.055kg/s and 0.0675kg/s for the two different inlet temperatures. Flow goes through a 7mm diameter nozzle, impinges on the heated part of the structure, side (AB)=16.5mm, and then is diverted sideways through a narrow channel of 1.8mm height at inlet and 0.9mm at exit.

III. RESULTS - DISCUSSION

Finite element calculations were performed on sections of the proposed divertor designs, using the commercially available fluid dynamics code FlowPlus, the fluid module of the COSMOS/M⁷ family of solvers. The code can solve in arbitrary geometry the thermal-fluid transport equations (Navier-Stokes plus energy) including a model for transport of fluid turbulence. There are several turbulence models available in the solver, and in this study the standard k-ε model was employed for the calculations.

Figures 1-2 show the schematic cross sectional views of the two divertor concepts. The cross sections labelled P1 to P6 depict the position for the velocity profiles shown in Figures 3-4. The contour (CD) marks the path followed for obtaining the wall and fluid temperatures, as well as the equivalent effective values of the heat transfer coefficient, shown in Figures 5-8. The effective heat transfer coefficient is based on the local heat transfer between solid and fluid and the fluid and wall temperatures, as calculated by the finite element analysis. General and bulk values of parameters for cases 1a, 2a, and 2b are given in Table I, as follows:

TABLE I
INLET AND OTHER FLOW AND HEATING PARAMETERS

Case	q_s (MW/m ²)	V_{inlet} (m/s)	T_{inlet} (°C)	Mass flow (kg/s)
1a	10.0	2.5	500.0	0.0901
2a	10.0	230.0	800.0	0.0549
2b	10.0	230.0	600.0	0.0676

The maximum values of the solid and solid in contact with the fluid temperatures, $T_{s(max)}$ and $T_{w(max)}$, respectively, the pressure drop ΔP and bulk temperature rise ΔT , inlet to exit, are given in Table II, as follows:

TABLE II
SURFACE, FLUID TEMPERATURES AND PRESSURE DROP

Case	$T_s^{(max)}$ (°C)	$T_w^{(max)}$ (°C)	ΔP (MPa)	ΔT (K)	T_{inlet} (°C)
1a	1366.9	1125.0	0.04935	254.67	500.0
2a	2047.2	1280.0	0.1631	30.41	800.0
2b	1795.0	1020.0	0.1992	25.03	600.0

The pressure drop for case 1a is entirely in the narrow section of the flow lined with the pins. For cases 2a-2b the pressure drop is mainly due to the constriction and occurs between the nozzle inlet and narrow channel inlet (location P2). Optimisation of the shape in the region around P2 will result in lower pressure drop values.

A comparison of the flow fields calculated for cases 2a and 2b, shows that the velocity distribution is insensitive to the increase of inlet temperature. Therefore, the pressure drop for the higher inlet coolant temperature is smaller and approximately in the proportion of the two temperatures ($1073.15/873.15=1.226\approx(0.1992/0.1631)$).

The variation of wall and fluid temperatures along the top of the narrow channel is shown in Figs. (5) and (7). For the design case 1a, the region of channel lined with the pins, in Fig. (5) from 1-6mm, due to the increased surface area for heat transfer, results in small differences between the wall and fluid temperatures, and large heat transfer values from the heated (top) side to the fluid. The result is very high values of the a posteriori calculated effective heat transfer coefficient, around $\sim 1100\text{kW/m}^2\text{-K}$ for that region. The temperature distribution results indicate that substantially lower temperatures are possible if channel lining with pins continues further downstream, and includes the region where the flow goes around the 90° bend. This might also be desirable to reduce any thermal stresses due to the $\sim 300\text{K}$ temperature rise immediately after the pin array region.

The wall and fluid temperatures for design cases 2a and 2b, shown in Fig. (7), exhibit a smooth variation along the flow direction, and the shape of the curves is similar with approximately 200K difference, reflecting the inlet temperature difference between the two cases.

The velocity profiles shown in Fig. (3) are representative of the flow in the P1-P6 locations. The profiles are scalar quantities of the velocity vector analysed in a direction normal and parallel to the orientation of the P1-P6 planes. The normalised distance is measured from the topside (heated) of the flow channel.

IV. CONCLUSIONS

The results of calculations show that the maximum temperatures on both designs are well within the operating limit of the structural material. Thermal-structural analysis is needed to provide answers to whether the material will withstand the stresses from internal pressure and induced temperature gradients. The retrospectively calculated effective heat transfer coefficients are higher than those predicted by empirical expressions found in the literature, thus the thermal results obtained previously can be thought to be conservative. The difference is entirely due to the specific flow patterns and induced turbulence observed in the geometries under consideration. The agreement of calculations with experimental values for similar conditions, inspires confidence in results from such calculations, and demonstrates that computational fluid dynamic finite element codes can accurately predict behaviour, and can be used to optimise the designs..

ACKNOWLEDGMENT

The author would like to thank Drs S Hermsmeyer (FZK) and A Pizzuto (ENEA) for supplying detailed information on the divertor designs. This work was supported by the UK Office of Science and Technology and EURATOM.

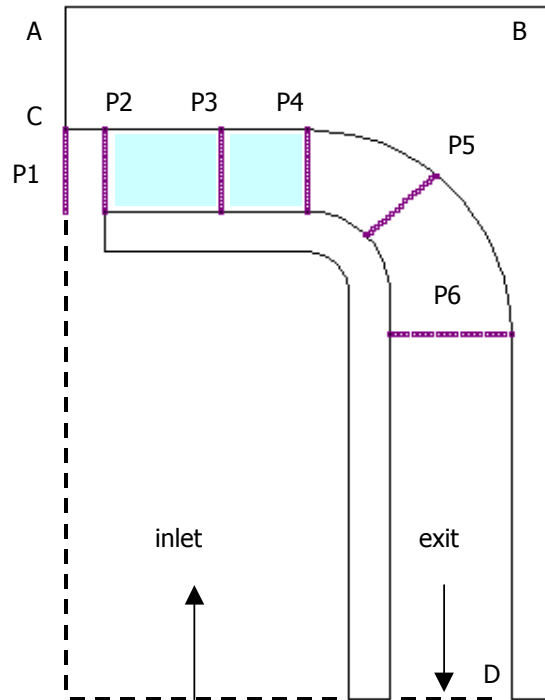


Fig.1: Schematic of the computational section used for the divertor design case 1a.

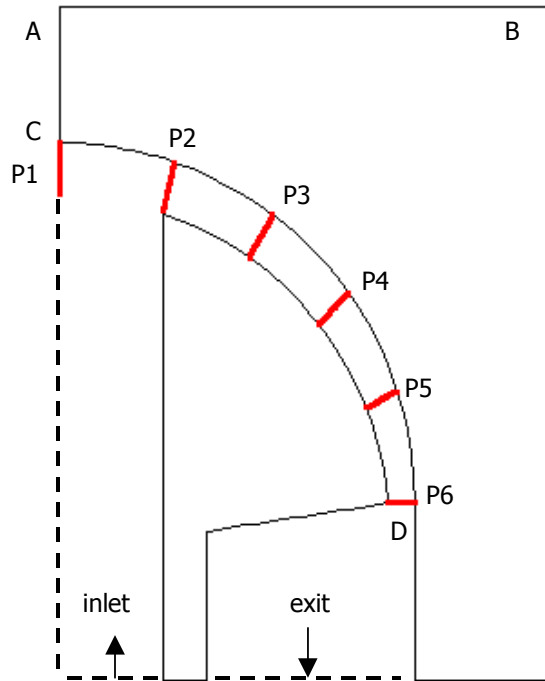


Fig.2: Schematic of the computational section used for the divertor design cases 2a and 2b.

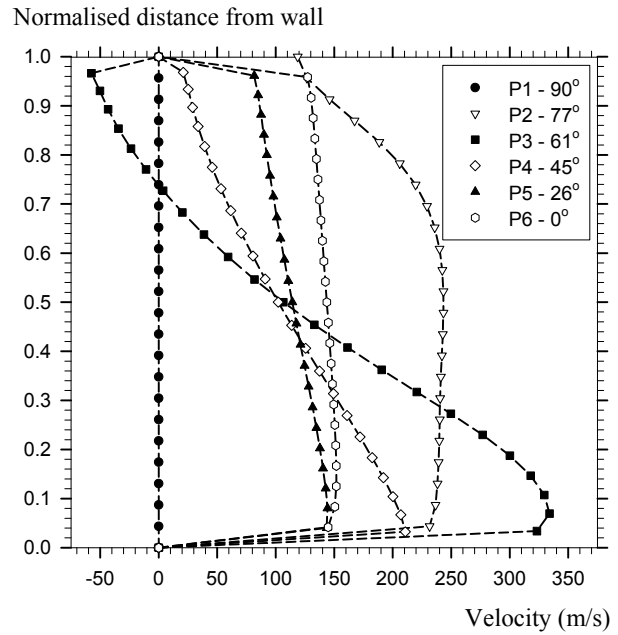


Fig. 4: Velocity profiles in the direction of the flow at various positions for the divertor design cases 2a and 2b.

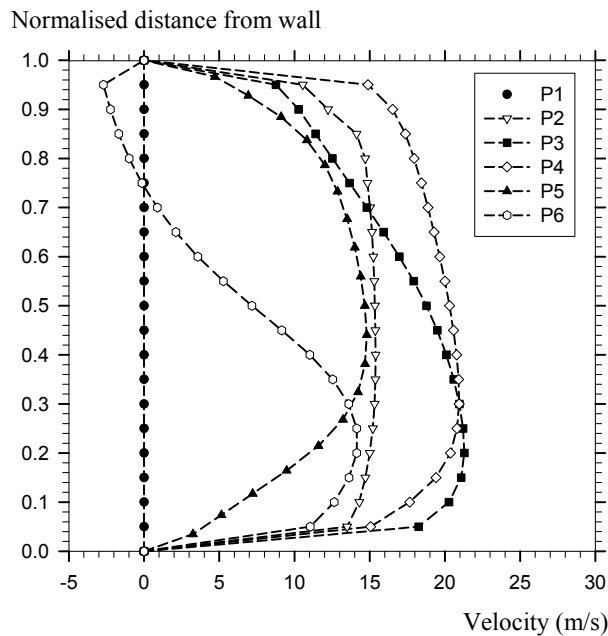


Fig. 3: Velocity profiles in the direction of the flow at various positions for the divertor design case 1a(pins).

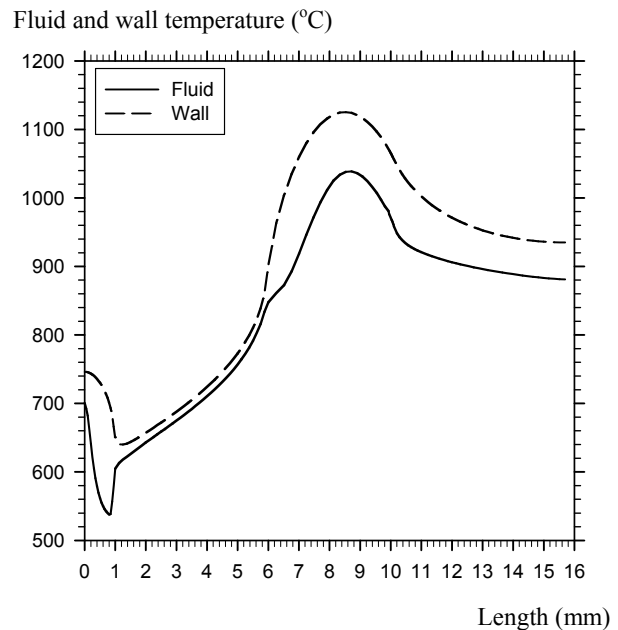


Fig. 5: Fluid and wall temperatures of the heated side exposed to the coolant, for the divertor design case 1a (pins).

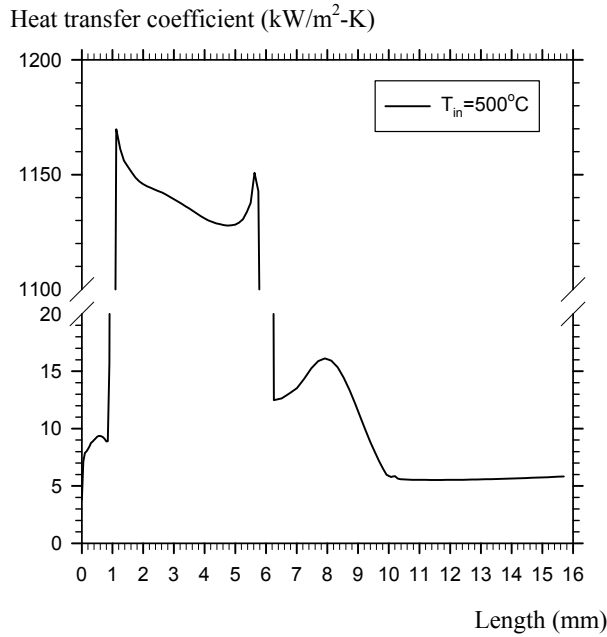


Fig. 6: Effective heat transfer coefficient for the divertor design case 1a(pins).

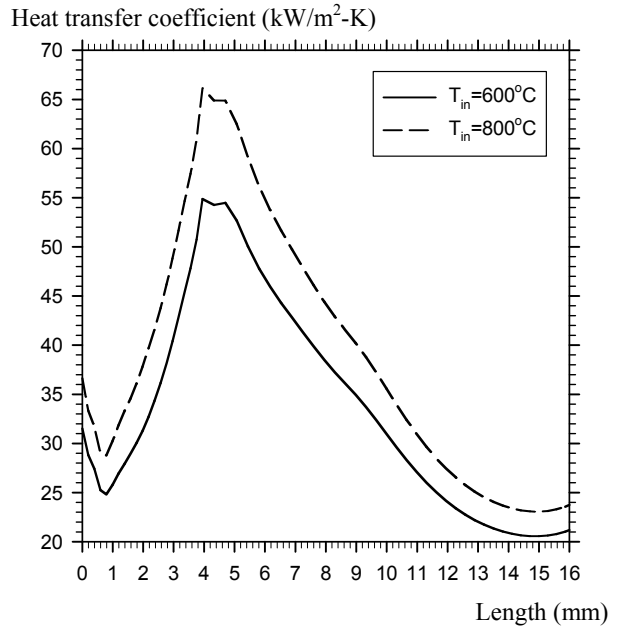


Fig. 8: Effective heat transfer coefficient for the divertor design cases 2a (inlet 800°C) and 2b (inlet 600°C).

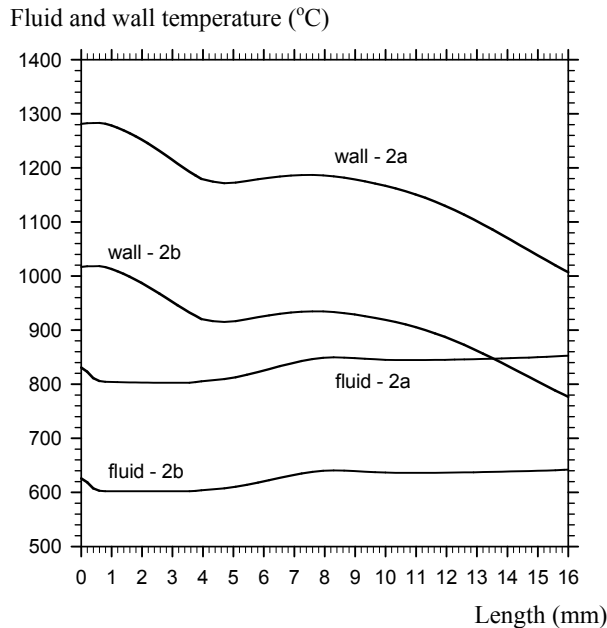


Fig. 7: Fluid and wall temperatures for the divertor design cases 2a (inlet 800°C) and 2b (inlet 600°C).

REFERENCES

1. S. HERMSMEYER, S. MALANG, ‘Gas-cooled high performance divertor for a power plant’, *Fusion Engineering and Design*, **61-62** (2002) 197-202.
2. A. PIZZUTO et. al., ‘Draft of Interim report for Task-PPCS-10: Alternative helium cooled divertor concept’, ENEA, Frascati, Italy (2002).
3. FP INCROPERA, DP DEWITT, ‘Fundamentals of heat and mass transfer’, John Wiley & Sons, New York, (1985).
4. BLUE RIDGE NUMERICS INC., ‘FlowPlus version 4.1: Solver user’s guide’, Raleigh, North Carolina, USA (2002).
5. JP HOLMAN, ‘Heat Transfer’, McGraw Hill, London, (1992).
6. A. PIZZUTO AND B. RICCARDI, ‘Preliminary Critical Heat Flux Assessment of The High Efficiency Thermal Shield Device’, *Private Communication*, November 2001.
7. STRUCTURAL RESEARCH AND ANALYSIS CORP., ‘COSMOS/M v2.6: A complete finite element analysis system’, Santa Monica, CA, USA (2000).